Modelling die filling for powders with complex rheology: A new DEM contact-model

T. Breinlinger, R. Schubert, A. Hashibon, T. Kraft

Fraunhofer IWM, 79108 Freiburg, Germany

Abstract

Die filling as the first step in the process chain of die compaction can already introduce various kinds of flaws like undesired density variations, which are difficult to repair later on. Predictive modelling of the complete die filling process including effects of powder handling history on rheology can assist in the optimization process to avoid such effects. However, the rheology of powders can be very difficult to model especially if heterogeneous agglomeration or time dependent consolidation effects occur as could be the case for powders containing organic binders. In this paper, we present a new discrete-element contact-force model that enables modelling complex powder flow characteristics including direct time dependent consolidation effects and load history dependent cohesion to describe the filling process of complex, difficult to handle powders.

Keywords

Powder, Die Filling, Simulation, DEM, Force Law

Introduction

The powder technological process chain consisting of die filling, compaction and sintering is an important technique in the manufacturing of sinter and hard metal components. In this process, deviations in the first steps can lead to undesirable properties of the final part. Looking in particular at the filling stage, introducing inhomogeneities like uneven density distributions or even completely unfilled regions in the die cavity can lead to unwanted part distortions after sintering or other flaws. During die filling, the kinematics (velocity and acceleration) of the filling shoe are important process parameters that affect both the powder flow rate and final density. This is particularly true for complex cohesive powders that may get agglomerated or consolidated during the initial stage, i.e., feeding the shoe and its consequent movement until the cavity is reached. Understanding and controlling the rheology of the powder during the whole filling process is therefore a key requirement for determining the optimal process parameters such as shape, acceleration and velocity of the shoe [1].

Predictive modelling of the complete filling process, including effects of powder handling history on the rheology, can assist in optimizing the whole manufacturing process. Numerous studies employing both

DEM and FEM have been successfully applied to model the behaviour of different powder filling and handling operations yielding valuable insight into the basic transport phenomena and the development of density inhomogeneity in the final parts (for more details and references see [2]). However, the vast majority of these studies assumes rather homogeneously flowing powders and exclude effects like sticking, time-dependent aging effects, caking and flow separation due to non-uniform residence times.

In this study, we propose a new model that explicitly adds time consolidation effects and also takes into account the effects of load history of the particles on the rate of increase or decrease of adhesion. It is based on a simple extension of the widely used Hertzian repulsion [3] and JKR cohesion [4] models by recognizing that the contact radius at zero load depends on the ratio between the contact interface energy and the effective stiffness of the material. We demonstrate that this new contact force model can be used to describe complex heterogeneous effects such as caking, sticking, intermittent agglomeration and non-uniform flow of powders.

History dependent DEM contact model

In DEM, the particles interact through an effective force field model which represents several types of contact forces acting between each pair of particles. In this study, we fit a specific contact force law to experimental observations, whereby the fitted contact force parameters should be taken as those of the effective coarse-scaled model (for details on scaling in DEM see [5]). Although several contact force models exists for cohesion and repulsion [6], they mostly differ in their functional form. Here we use those models that include Hertzian repulsion $\boldsymbol{F}^{rep}$ [3], JKR cohesion $\boldsymbol{F}^{coh}$ [4] and viscous damping effects $\boldsymbol{F}^{vis}$ [7] between the effective DEM particles as defined by

$$\boldsymbol{F}^{rep} = \left(\frac{2}{3}\tilde{E}\sqrt{\tilde{R}}\; h_{ij}^{2/3}\right)\hat{\boldsymbol{r}}_{ij} \tag{1}$$

$$\boldsymbol{F}^{coh} = -\left(\sqrt{4\pi w\tilde{E}}\;\; \tilde{R}^{3/4}\;\; h_{ij}^{3/4}\right)\hat{\boldsymbol{r}}_{\boldsymbol{ij}} \tag{2}$$

$$\boldsymbol{F}^{vis} = -\left(\gamma_n\sqrt{\tilde{R}\; h_{ij}}(\boldsymbol{v}_i - \boldsymbol{v}_j)\cdot\hat{\boldsymbol{r}}_{\boldsymbol{ij}}\right)\hat{\boldsymbol{r}}_{\boldsymbol{ij}} \tag{3}$$

where $\boldsymbol{h_{ij}} = \boldsymbol{R_i} + \boldsymbol{R_j} - |\boldsymbol{r_{ij}}|$ is the overlap of particles $\boldsymbol{i}$ and $\boldsymbol{j}$ at positions $\boldsymbol{r}$ having radii $\boldsymbol{R}$ and $\boldsymbol{r_{ij}} = \boldsymbol{r_i} + \boldsymbol{r_j}$. $\tilde{\boldsymbol{R}} = \frac{\boldsymbol{R_i R_j}}{(\boldsymbol{R_i}+\boldsymbol{R_j})}$ is the effective particle radius and $\tilde{\boldsymbol{E}} = \frac{\boldsymbol{E}}{(\boldsymbol{1}-\boldsymbol{\nu}^{\boldsymbol{2}})}$ is the effective stiffness, $\boldsymbol{E}$ is the Young's modulus and $\boldsymbol{\nu}$ is the Poisson ratio, $\boldsymbol{w}$ is the cohesive energy density, $\boldsymbol{\gamma_n}$ is the contact viscosity (taken as an empirical damping parameter) and $\boldsymbol{v}$ is the particle velocity.

The consolidation of the powder, i.e. the time dependence of the cohesion, is taken into account by increasing the surface energy $\boldsymbol{w}$ of the contact and, at the same time, scaling the effective stiffness in the same manner so that the ratio $\boldsymbol{w}/\tilde{\boldsymbol{E}}$ remains constant. In this way the point of zero contact force or equilibrium inter-particle overlap $\boldsymbol{h_0}$ remains constant throughout the simulation, while the adhesion increases. In other words, the increase of adhesion is decoupled from the deformation in our model.

In our proposed model the scaling of the surface energy and the effective stiffness are assumed to be a function of an effective loading-time. More specifically, we assume that the scaling factor is a linear function of the effective loading-time, which is given through a time integral over the particle-particle overlap $\boldsymbol{h_{ij}}$, see Figure 1(a). We first introduce an effective normalized and capped overlap parameter $\boldsymbol{h^*}$ as

$$h^* = \begin{cases} {h}/{h_0} - 1, & 0 < h \leq 2h_0 \\ 1, & h > 2h_0 \end{cases}, \quad (4)$$

where $\boldsymbol{h_0}$ is the equilibrium overlap between the grains, which is given by

$$h_0 = \left(\frac{9}{2}\pi\frac{w}{\tilde{E}}\right)^{\frac{2}{3}} \tilde{R}^{\frac{1}{3}}. \quad (5)$$

The overlap parameter $\boldsymbol{h^*}$ is shown schematically in Fig. 1(b). The effective overlap is negative when the particles are in the cohesive region ($\boldsymbol{0 < h \leq h_0}$) and positive in the repulsive region ($\boldsymbol{h > h_0}$). The capping is employed to limit an excessive unrealistic effective overlap due to a continuous load of the particles. This does not constitute a limitation of the model as the capping at $\boldsymbol{2h_0}$ is a parameter of the model that can be varied. Then we define an effective loading-time of the contact $\boldsymbol{\tau}$ as an integral over $\boldsymbol{h^*}$ throughout the whole contact duration time $\boldsymbol{T}$

$$\tau = \begin{cases} \int_0^T h^* dt, & \tau < \tau_{max} \\ \tau_{max}, & \tau \geq \tau_{max} \end{cases}. \quad (6)$$

Due to this integration, the effective loading-time parameter $\boldsymbol{\tau}$ includes information on the contact load history, i.e. loading of the particle contact and the duration of contact simultaneously. Eq. 6 indicates that the higher the compressive load ($\boldsymbol{h > h_0}$) the more the loading time increases, while during tensile loading ($\boldsymbol{0 < h \leq h_0}$) the effective loading time decreases. The effective loading time is capped by the relaxation time parameter $\boldsymbol{\tau_{max}}$, which is another new model parameter. Finally, we introduce a scaling factor $\boldsymbol{\alpha(\tau)}$ for the Young's modulus and cohesion that is active only in the cohesive domain ($\boldsymbol{0 < h \leq h_0}$) and given as a linear function of the effective loading-time as

$$\alpha(\tau) = \begin{cases} \dfrac{\alpha_{max} - 1}{\tau_{max}} \cdot \tau + 1, & \tau < \tau_{max} \\ \alpha_{max}, & \tau \geq \tau_{max} \end{cases} \quad (7)$$

where $\boldsymbol{\alpha_{max} \geq 1}$ is a parameter setting the maximum possible scaling at $\boldsymbol{\tau_{max}}$ as shown in Figure 1(c). Several functions could be used instead of the linear capped scaling factor in Eq. 7, for example an exponential function, which would lead to different loading and unloading rates. However, for simplicity the capped linear form is chosen here as it enables a more straightforward analysis of the dependence of the contact on the parameters $\boldsymbol{\tau_{max}}$ and $\boldsymbol{\alpha_{max}}$, which become two additional contact force parameters. Fig. 1(d) shows a schematic of the new contact force model taking history dependent cohesion effects into account (green) in comparison to a non-scaled Hertz-JKR model (black). We limit the application of the scaling to the regime of tensile contacts, i.e., to whenever $\boldsymbol{0 < h \leq h_0}$ so as to preserve the repulsive branch for $\boldsymbol{h > h_0}$ as shown schematically in Figure 1(d). This simple modification to the contact force model allows controlling the behaviour of the powder under different conditions in an intricate but subtle manner.

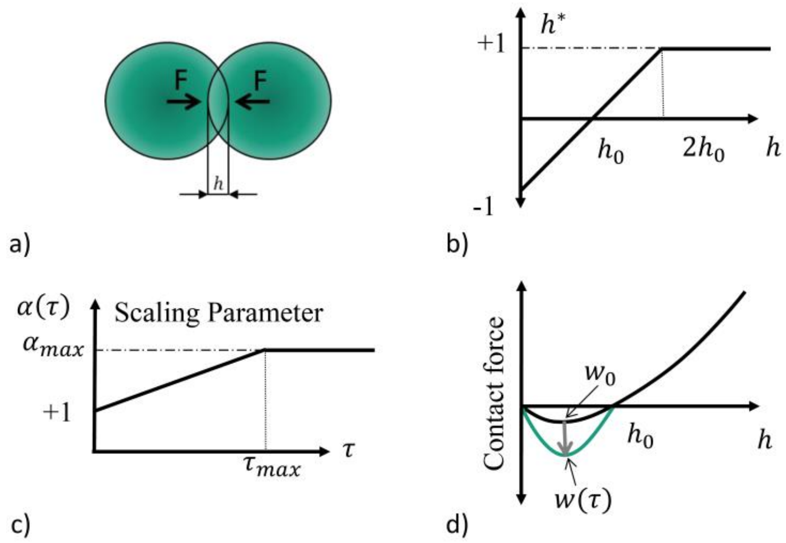

Figure 1: A schematic showing the particle overlap h (a), the effective overlap parameter h* (b), the scaling parameter α (c), and the resulting scaled contact force model (d).

Application to industrially relevant filing processes

As a demonstration for the possibilities of the new model we use the new contact force model to describe a particularly difficult to handle powder. As the original powder is quite fine, it cannot be directly modelled with DEM particles of the actual grain size. Instead, we applied an initial coarse-graining of all particles. The limit of coarse scaling is usually given by the smallest geometrical feature in the system, which in this case is the width of the cavity inside the die. For more details of the powder see [2]. Reference filling experiments were carried out at Fraunhofer IKTS using the FlowD [8] setup, which was designed to be as close as possible to industrial applications. High quality imaging makes it possible to compare the filling process with our model predictions.

For the simulations, the experimental geometry of the reference system was used. The filling simulations were conducted using the particle based simulation package SimPARTIX® [9]. In addition to the filling shoe, the feeding hose and silo were also included in the simulation model (Fig. 2). This allows a more close reproduction of the whole process including the preparation of the powder in the shoe that can affect consolidation time and clogging of the powder. The goal is to be able to take these effects into account using the new developed contact force model. The movement profile of the shoe was set in the simulations to exactly match that performed in the experiments. Depending on the level of grain coarsening used in order to speed up simulation times and filling shoe velocity typical calculation times had been in the order of one to several days on a Linux workstation.

The investigated powder shows a peculiar splitting of the discharge flow as shown in Figure (a). This splitting could not be easily reproduced in the modelling employing the standard JKR-Hertz contact force model. The splitting appears to be a result of some kind of heterogeneous agglomeration or caking of the powder that occurs during the initial filling of the show from the silo and consequently the movement of the shoe as a whole, without substantial movement of the powder inside the bulk of the shoe. This hints that a model that takes into account consolidation and load dependent agglomeration of the powder as that proposed here is needed.

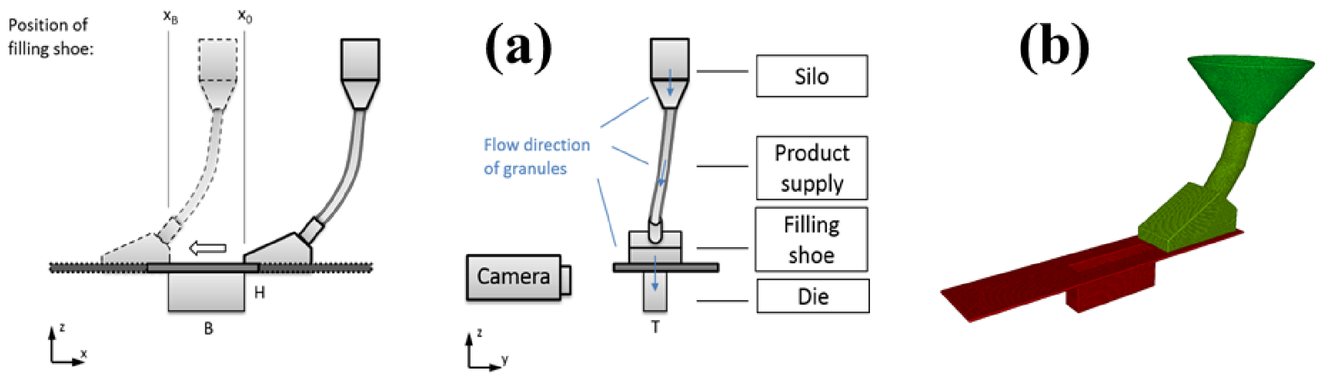

Figure 2: Experimental FlowD [8] setup in (a) featuring transparent shoe and a high speed camera system. The corresponding modelling system using particle walls is shown in (b). The dimensions of the cavity (in both experiments and simulations) are: B = 7 cm, H = 3 cm and T = 1.5 cm. The width of the shoe is 3.5 cm.

One set of filling experiments with a final shoe velocity of v = 0.36 m/s was chosen to fit the time dependent contact force model. The fitting was carried out via the variation of the model parameters E, ν, w, τ_{max}, and α_{max}. For more details see [2].

Figure shows a comparison of two snapshot images of both experiment (left) and simulation (right) for two different stages in time during the die filling process. Figure (a) and (b) show the filling process after about 40 % of shoe passage. In the experiment, we observed a complex flow pattern featuring two different zones of powder flow (highlighted by yellow arrows in the figure) that separate from each other and move as individual powder streams. Comparing this with the simulation results using the new contact force model and with the best fit contact parameters, it can be seen that this separation of different zones can be well reproduced. In Figure (c) and (d) the flow pattern just after completion of the shoe's passage is shown. As indicated by the wave like surface, the powder is in a dynamic, fluidized state of motion at this stage. Again, there is good visual qualitative agreement between experiment and simulation also at this late stage of the die filling process. A quantitative difference can be seen in the amount of powder in the lower jet (Figure (a) vs. (b)), which is believed to be due to the coarse graining as the model particles are much larger than the individual powder grains.

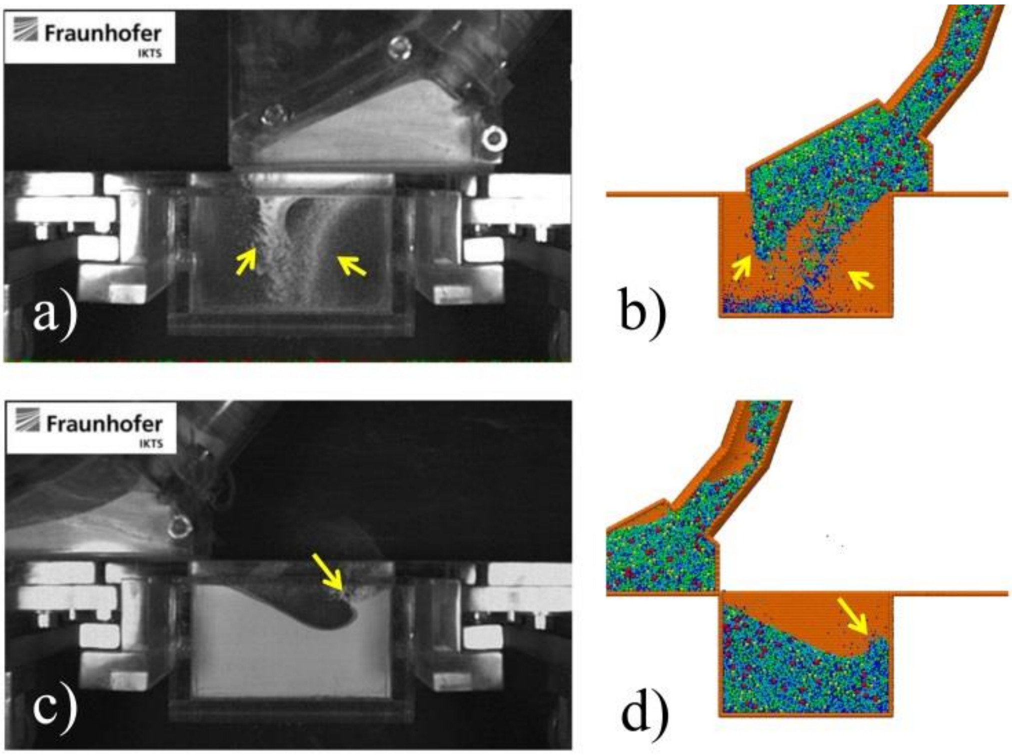

Figure 3: Experimental and simulation results for die filling featuring complex flow patterns such as flow separation (a, b) and fluidization (c, d).The simulation results are made with the best fit history dependent cohesion model. See text for details.

Summary

We presented a new contact force model that takes into account both load dependence and time dependence of the contact model for granular flows. It is based on the classic Hertz-JKR model and allows for both up- and down-scaling of the cohesive inter particle contact force on an arbitrary time scale as a function of the load history. With this new model it is possible to describe granular flow processes of complex cohesive powders in die filling technological applications even without taking into account static friction. It is particularly suitable for cases where the apparent cohesion of the powder, i.e. its ability to stick together in chunks rather than to flow smoothly, may change as a response to external conditions (for example due to friction and shear with static walls, or simply different residence times during handling). The scaling of the Young’s modulus in our model is based on the assumption that increasing the surface adhesion will also result in stiffer bonds. The relaxation time associated with the rate of increase or decrease of the contact adhesion and stiffness is related to the load history, and can result in either stiffer more cohesive bond for contacts under extended compression, or to free flowing powders when the compressive stresses diminish.

The results clearly illustrate that the proposed history dependent contact force model is capable of reproducing even a peculiar splitting of the discharge flow as observed experimentally, at least for the specific powder and experimental setup presented here. However, one cannot exclude that air flow may also play an important part or that the coarse graining and cohesion of the powders can also be suspect reasons.

Despite its simplicity, the proposed new contact force model is very similar to the well-known JKR and Hertz models and extends them to take into account the history of the loading in an intricate manner. It can also be extended further to take into account plastic deformations by allowing different scaling for the Young's modulus and cohesion. The model can be augmented with static, sliding and rolling friction models but this was not the main focus in the present study. Therefore, further investigation on the interplay of friction and load history dependent cohesion is required.

Acknowledgement

This work has been funded by the Federal Ministry of Economics and Technology (BMWi) via the German Federation of Industrial Research Associations „Otto von Guericke" e.V. (AiF) (IGF-Nr.: 430 ZBG).

References

1. Z. Guo, X. Chen, H. Liu et al., Fuel Process. Technol. 125 (2014) 59–66
2. A. Hashibon, R. Schubert, T. Breinlinger and T. Kraft, Comp. Particle Mech. 3 (2016) 437–448
3. H. Hertz, J. Reine Angew. Math. 92 (1881) 156–171
4. K.L. Johnson, K. Kendall and A.D. Roberts, Proc. R. Soc. Lond. A 324 (1971) 301–313
5. C. Bierwisch, T. Kraft, H. Riedel and M. Moseler, J. Mech. Phys. Solids 57 (2009) 10–31
6. J. Tomas, Part. Sci. Technol. 19 (2001) 95–110
7. L.D. Landau, L.P. Pitaevskii, A.M. Kosevich and E.M. Lifshitz, Theory of Elasticity, Elsevier, Amsterdam (1986)
8. B. Glöß and M. Fries, cfi/Ber. DKG 93 (10) (2016) E38-E43
9. http://www.simpartix.com